



## Anti-adipogenic activity of maackiain and ononin is mediated *via* inhibition of PPAR $\gamma$ in human adipocytes

Saveta G. Mladenova<sup>a,1</sup>, Martina S. Savova<sup>b,c,1</sup>, Andrey S. Marchev<sup>b,c</sup>, Claudio Ferrante<sup>d</sup>, Giustino Orlando<sup>d</sup>, Martin Wabitsch<sup>e</sup>, Milen I. Georgiev<sup>b,c,\*</sup>

<sup>a</sup> BB-NCIPD Ltd., BB-National Centre of Infectious and Parasitic Diseases, Ministry of Health, 1000 Sofia, Bulgaria

<sup>b</sup> Department of Plant Cell Biotechnology, Center of Plant Systems Biology and Biotechnology, 4000, Plovdiv, Bulgaria

<sup>c</sup> Laboratory of Metabolomics, Department of Biotechnology, The Stephan Angeloff Institute of Microbiology, Bulgarian Academy of Sciences, 139 Ruski Blvd, 4000 Plovdiv, Bulgaria

<sup>d</sup> Department of Pharmacy, G. d'Annunzio University, 66100 Chieti, Italy

<sup>e</sup> Division of Pediatric Endocrinology and Diabetes, Department of Pediatrics and Adolescent Medicine, Ulm University Medical Center, 89073 Ulm, Germany

### ARTICLE INFO

#### Key words:

Obesity  
Adipogenesis  
PPAR $\gamma$   
*Ononis spinosa* L.  
Ononin  
Maackiain

### ABSTRACT

Obesity is a global health burden for which we do not yet have effective treatments for prevention or therapy. Plants are an invaluable source of bioactive leads possessing anti-adipogenic potential. Ethnopharmacological use of *Ononis spinosa* L. roots (OSR) for treatment of obesity and metabolic disorders requires a scientific rationale. The current study examined the anti-adipogenic capacity of OSR and its secondary metabolites ononin (ONON) and maackiain (MACK) in human adipocytes as an *in vitro* model of obesity. Both ONON and MACK diminished lipid accumulation during adipocyte differentiation. Molecular docking analysis exposed the potential interactions between MACK or ONON and target regulatory adipogenic proteins. Furthermore, results from an RT-qPCR analysis disclosed significant upregulation of AMPK by MACK and ONON treatment. In addition, ONON increased *SIRT1*, *PI3K* and *ACC* mRNA expression, while MACK notably downregulated *CEBPA*, *AKT*, *SREBP1*, *ACC* and *ADIPOQ*. The protein level of PI3K, C/EBP $\alpha$ , PPAR $\gamma$  and adiponectin was reduced upon MACK treatment in a concentration-dependent manner. Similarly, ONON suppressed PI3K, PPAR $\gamma$  and adiponectin protein abundance. Finally, our study provides evidence that ONON exerts anti-adipogenic effect by upregulation of *SIRT1* and inhibition of PI3K, PPAR $\gamma$  and adiponectin, while MACK induced strong inhibitory effect on adipogenesis *via* hampering PI3K, PPAR $\gamma$ /C/EBP $\alpha$  signaling and anti-lipogenic effect through downregulation of *SREBP1* and *ACC*. Even though OSR does not hamper adipogenic differentiation, it could be exploited as a source of natural leads with anti-adipogenic potential. The multidirectional mechanism of action of MACK warrant further validation in the context of *in vivo* obesity models.

### 1. Introduction

Obesity is generally defined as an abnormal fat accumulation that

derives from a positive energy balance and a complex combination of genetic and behavioural factors. The constant increase in obesity rates highlights the pathology as a serious health burden [1–3].

**Abbreviation:**  $\Delta$ G, binding free energy; ACC, acetyl-CoA carboxylase; ADIPOQ, adiponectin-coding gene; AKT, protein kinase B; AMPK, adenosine monophosphate-activated protein kinase; C/EBP $\alpha$ / $\beta$ / $\delta$ , CCAAT-enhancer-binding protein alpha/beta/delta; FABP4, fatty acid binding protein 4; FAS, fatty acid synthase; COSY, homonuclear correlation spectroscopy; HSQC, heteronuclear single quantum coherence spectroscopy; IGF-1, insulin-like growth factor 1; Ki, affinity constant; MACK, maackiain; MAPK, mitogen-activated protein kinase; NF- $\kappa$ B, nuclear factor kappa-light-chain-enhancer of activated B cells; NMR, nuclear magnetic resonance; ONON, ononin; OSR, *Ononis spinosa* L. root extract; PPAR $\gamma$ , peroxisome proliferator-activated receptor gamma; PI3K, phosphoinositide 3-kinase; PDB, protein data bank; RPL13A, ribosomal protein L13a; SGBS, Simpson-Golabi-Behmel syndrome; SIRT1, sirtuin-1; SREBP1, sterol regulatory element-binding protein 1; TSPA-*d*<sub>4</sub>, 3-(trimethylsilyl)propionic-2,2,3,3-*d*<sub>4</sub>; TUBB,  $\beta$ -tubulin.

\* Corresponding author: Laboratory of Metabolomics, Department of Biotechnology, The Stephan Angeloff Institute of Microbiology, Bulgarian Academy of Sciences, 139 Ruski Blvd, 4000 Plovdiv, Bulgaria.

E-mail address: [milengeorgiev@gbg.bg](mailto:milengeorgiev@gbg.bg) (M.I. Georgiev).

<sup>1</sup> Equal contribution.

<https://doi.org/10.1016/j.bioph.2022.112908>

Received 17 February 2022; Received in revised form 21 March 2022; Accepted 29 March 2022

Available online 1 April 2022

0753-3322/© 2022 The Author(s).

Published by Elsevier Masson SAS. This is an open access article under the CC BY-NC-ND license (<http://creativecommons.org/licenses/by-nc-nd/4.0/>).

Obesity-related complications such as cardiovascular disease, metabolic syndrome, type 2 diabetes, different types of cancer and osteoarthritis, substantially impair the quality of life of the patients, aggravate the economic weight on society and increase the mortality every year [3,4].

Approved anti-obesity medicines have limited efficacy and numerous side effects, such as abdominal pain, diarrhoea, insomnia and nausea [5]. Multiple investigations suggest that the natural products may have immense anti-obesity potential with insignificant side effects observed [6,7]. Therefore, identification of novel natural compounds that prevent abnormal lipid accumulation and clarification of their mechanism of action are essential for introduction of safe and effective plant-based therapeutic options for obesity management.

Different modes of action are attributed to the anti-obesity activity of plant extracts and natural compounds such as inhibition of adipogenesis and/or lipogenesis, stimulation of lipid hydrolysis paired with enhanced mitochondrial oxidation of released fatty acids, and a decrease in chronic low-grade inflammation which is characteristic for obesity [2, 8]. Substantial advantages of the plant-based products are the potential complexity of their anti-obesity effect, which may involve multiple of above-mentioned mechanisms. The contemporary understanding of the complex coordination of the transformation of preadipocytes into mature adipocytes has identified molecular targets that could be therapeutically exploited [9,10]. A possible mechanism for management of excess adiposity is inhibition of the phosphoinositide 3 kinase (PI3K)/protein kinase B (AKT) signaling pathway engaged in adipogenesis initiation [9,11–14]. Another approach is the downregulation of the key transcription factors responsible for the terminal adipocyte differentiation such as peroxisome proliferator-activated receptor gamma (PPAR $\gamma$ ), CCAAT-enhancer-binding protein alpha (C/EBP $\alpha$ ) and sterol regulatory element-binding protein 1 (SREBP1) [15,16]. The intracellular sensor that controls cellular energy balance, adenosine monophosphate (AMP)-activated protein kinase (AMPK), modulates metabolic processes through phosphorylation of proteins responsible for lipid metabolism, fatty acid oxidation, glucose uptake, and serves as a target for anti-obesity compounds [17,18]. Activation of AMPK through phosphorylation inhibits the initiation of adipogenic differentiation by a decrease in the expression of C/EBP $\beta$  and  $\delta$ , followed by negative regulation of PPAR $\gamma$ , C/EBP $\alpha$  and late adipogenic markers such as acetyl-CoA-carboxylase (ACC), fatty acid synthase (FAS), fatty acid binding protein 4 (FABP4), and the primary transcriptional regulator of lipogenesis SREBP1 [15]. Another regulator of gene expression and metabolic activity that is dependent on the cellular energy state is the family of sirtuins, which are highly conserved histone NAD-dependent deacetylases and/or ADP ribosyl transferases. Sirtuin 1 (SIRT1) has been reported to play an essential role in adipocyte differentiation, where its upregulation is associated with repression of adipogenesis mediated by inhibition of PPAR $\gamma$  transcriptional activity [19,20]. In addition, decreased activity of SIRT1 is associated with adipocyte hyperplasia and aggravated inflammation in the context of obesity [21].

*Ononis spinosa* L. is a perennial plant with a woody base and is widely spread in Europe. The phytochemical profile of *O. spinosa* root extract (OSR) consists of wide range of secondary metabolites, such as iso-flavones, saponins, terpenes, etc. [22]. In traditional medicine *O. spinosa* is used for treatment of inflammation of the urinary tract and kidney stones [23], as well as for its laxative and wound healing effects [24]. Diverse biological activities have been described for *O. spinosa* extracts such as antibacterial, antifungal, inhibiting hyaluronidase-1 [23], anti-inflammatory activity by inhibiting the 5-lipoxygenase [24] and the Toll-like receptor 4 signaling pathway [25]. Despite the absence of scientific literature regarding the anti-adipogenic effect of OSR, in Bulgarian ethnopharmacology the roots are used as a component of anti-obesity herbal combinations.

In the current study the anti-adipogenic potential of OSR and selected pure compounds, namely, ononin (ONON) and maackiain (MACK), was investigated. Both compounds were selected following targeted NMR-based metabolite profiling of the extract. *In silico* docking

analysis was performed to evaluate the molecular interaction between selected secondary metabolites and adipogenic regulatory proteins. Influence on adipogenesis and lipolysis upon OSR, ONON and MACK treatment was investigated *in vitro* in differentiated human adipocytes. Further clarification of the molecular mechanism of the observed bioactivity was assessed by analyses of the relative mRNA and protein expression of crucial adipogenic transcription factors.

## 2. Materials and methods

### 2.1. Materials

Pure ONON, chemical name: 3-(4-methoxyphenyl)-7-[(2 S,3 R,4 S,5 S,6 R)– 3,4,5-trihydroxy-6-(hydroxymethyl)oxan-2-yl]oxochromen-4-one, molecular weight 430.4 g/M purity  $\geq$  95% HPLC; #82359) and MACK, chemical name: (1 R,12 R)– 5,7,11,19-tetraoxapenta-cyclo [10.8.0.0<sup>2,10</sup>.0<sup>4,8</sup>.0<sup>13,18</sup>]icosa-2,4(8),9,13(18),14,16-hexaen-16-ol, molecular weight 284.26 g/M; purity  $\geq$  95% HPLC; #83103) were supplied from Phytolab (Vestenbergsgreuth, Germany). Deuterated water and methanol were provided by Deutero GmbH (Kasbellaun, Germany). Standard chemicals, culture media and its constituents were supplied from Merck KGaA (Darmstadt, Germany). Reagents and consumables for gel electrophoresis, immunoblotting and RT-qPCR analyses from Bio-Rad Laboratories, Inc. (Hercules, CA, USA) were used. Western blotting antibodies were used as follows: rabbit anti-C/EBP $\alpha$  (#2295), anti-PPAR $\gamma$  (#2443); anti-AKT (#9272), anti-PI3K (#4257), anti-AMPK (#5831) and anti-phosphorylated AMPK (pAMPK, #2535) from Cell Signaling Technology (Leiden, Netherlands); anti-adiponectin (#GTX112777) from GeneTex Inc. (Irvine, CA, USA); hFAB Rhodamine anti-actin beta (#12004164) and anti-tubulin (#12004166) antibodies and secondary StarBright Blue 700-conjugated goat anti-rabbit IgG (#12004162) from Bio-Rad.

### 2.2. Collection and extraction of *O. spinosa* roots

The roots from *O. spinosa* were collected in 2018 from the village Dedovo, Bulgaria in the Rhodope mountains (latitude: 41°59'38"N; longitude: 24°39'26"E), identified and characterized by Dr. Andrey S. Marchev. After freeze-drying the plant material was ground and stored at – 20 °C. Aqueous methanol solution (50%) was used for single ultrasound-assisted extraction (1:30 w/v) for 20 min at 20 °C. A rotary vacuum evaporator was used to concentrate the crude liquid extract at 40 °C. The prepared OSR dry extract was kept frozen prior to further analysis.

### 2.3. NMR-based metabolite profiling

Nuclear magnetic resonance (NMR) analysis was performed according to the protocol described by [26]. In brief, 10 mg of the obtained extract was dissolved in equal amounts of 0.4 mL CD<sub>3</sub>OD and D<sub>2</sub>O, containing KH<sub>2</sub>PO<sub>4</sub> buffer with pH 6.0 and 3-(trimethylsilyl)propionic-2,2,3,3-*d*<sub>4</sub> (TSPA-*d*<sub>4</sub>) as an internal standard at final concentration of 0.005% (w/v). The <sup>1</sup>H NMR and 2D <sup>1</sup>H–<sup>1</sup>H homonuclear correlation (<sup>1</sup>H–<sup>1</sup>H COSY) and heteronuclear single quantum coherent (HSQC) spectra were obtained on a Bruker AVII+ 600 spectrometer (Bruker, Karlsruhe, Germany), operating at 25 °C, 600.13 MHz proton frequency, with 4.07 s relaxation time and CD<sub>3</sub>OD as an internal lock. The obtained spectra were automatically reduced to ASCII files using AMIX software (version 3.7, Bruker), phased, base line corrected and referenced at 0.0 ppm to the internal standard TSPA-*d*<sub>4</sub> using MestReNova software v. 12.0.0 from Mestrelab Research (Santiago de Compostela, Spain). All signals were normalized in relation to the peak of TSPA-*d*<sub>4</sub> and scaled to 1.0.

#### 2.4. Cell culture and treatment

Human preadipocyte cell strain Simpson-Golabi-Behmel syndrome (SGBS) was cultivated following the optimal conditions. When preadipocytes reached confluence, differentiation was initiated as described early [27]. During the differentiation process treatment with OSR (5, 10 and 25 µg/mL), pure ONON (5, 10 and 25 µM), MACK (5, 10, 25 and 50 µM) or 0.02% DMSO as vehicle was applied. Selected time points of treatment were day 0, 4 and 8 of differentiation. Applied concentrations were selected upon toxicity evaluation through cell viability assay (Fig. S1). The highest concentration of MACK 50 µM was included based on the strong and concentration-dependent reduction of lipid accumulation within the range of 5–25 µM that was not observed upon ONON or OSR treatments.

Lipid staining was performed, culture media samples for determination of glycerol concentration were collected, and protein samples were isolated on the day 9th of differentiation. Total RNA samples were obtained to evaluate alternations in gene expression on the day 3rd and 9th of differentiation. All *in vitro* assays were performed in three independent experiments.

#### 2.5. In silico molecular docking

Computational predictions of the molecular interactions between the selected pure compounds and target protein structures were conducted through the Autodock Vina of the PyRx software package as described elsewhere [26]. The protein crystal structures were derived from the protein data bank (PDB, [www.wwpdb.org](http://www.wwpdb.org)). Each compound was tested through Autodock4 and Lamarckian genetic algorithms to dock 250 conformations (Molinspiration Database, [www.molinspiration.com](http://www.molinspiration.com)). The images of the protein to ligand non-bonding interactions were processed on a Discovery studio 2020 Visualizer.

#### 2.6. Evaluation of lipid accumulation and glycerol release

Lipid staining with Oil red O dye was performed as described previously [28]. Visualization of lipid droplets in differentiated adipocytes was done using an Oxion Inverso OX.2053-PLPH inverted microscope equipped with DC.10000-Pro CMEX camera from Euromex (Arnhem, The Netherlands). The optical density of extracted lipid dye was measured at 495 nm on Biochrome Anthos Zenyth 340 multiplate reader (Cambridge, UK) and the quantity of the accumulated lipids in different groups was calculated as a percentage, compared to the vehicle-treated controls.

The basal lipolysis was assessed by determination of the glycerol concentration (µM) released in the culture media. Adipolysis assay kit (#MAK313) from Merck KGaA was employed and the manufacturer's procedure was strictly implemented.

#### 2.7. RT-qPCR analysis

Extraction of the total RNA was performed with Quick-RNA miniprep kit (#R1055) from Zymo Research (Irvine, CA, USA). Reverse transcription was made with First strand cDNA synthesis kit (#PR008-XL), Canvax (Córdoba, Spain). The RT-qPCR analysis was conducted on the C1000 Touch thermal cycler with CFX96 detection system (Bio-Rad) using SsoFast EvaGreen Supermix (#1725204, Bio-Rad). A comparative threshold cycle ( $\Delta\Delta C_t$ ) method was applied for quantification of relative gene expression using CFX Maestro software (Bio-Rad), as reference genes were used ribosomal protein L13a (*RPL13A*) and  $\beta$ -tubulin (*TUBB*). Primers used in the present study are listed in Table S1.

#### 2.8. Western blotting

Total protein extraction with ice-cold RIPA lysis buffer supplemented with 1% protease phosphatase inhibitors and quantification were

performed as described in details previously [26]. Equal amounts of total protein lysates were resolved on a 10% sodium dodecyl sulphate polyacrylamide gel and transferred to polyvinylidene fluoride membranes. After blocking for an hour at room temperature with 5% (w/v) skim milk in Tris buffered saline, overnight incubation with primary antibodies against the selected proteins (C/EBP $\alpha$ , PPAR $\gamma$ , AKT, PI3K, AMPK and pAMPK) was done overnight. A multiplex fluorescent detection was visualized on a ChemiDoc MP Imaging System (Bio-Rad). Normalization of the protein abundance was performed against  $\beta$ -actin or  $\beta$ -tubulin as housekeeping proteins using Image Lab 6.0.1 software (Bio-Rad). Whole images of the original Western blots are provided on Fig. S2.

#### 2.9. Statistical analysis

Statistical analysis was performed in SigmaPlot v11.0 from Systat Software GmbH (Erkrath, Germany) and the data were represented as mean  $\pm$  SEM. Variations between the groups were calculated by one-way analysis of variance (ANOVA) followed by Bonferroni's *post hoc* test. The level of statistical significance was set at \* $p < 0.05$ .

### 3. Results

#### 3.1. Metabolite identification through NMR-based spectroscopy

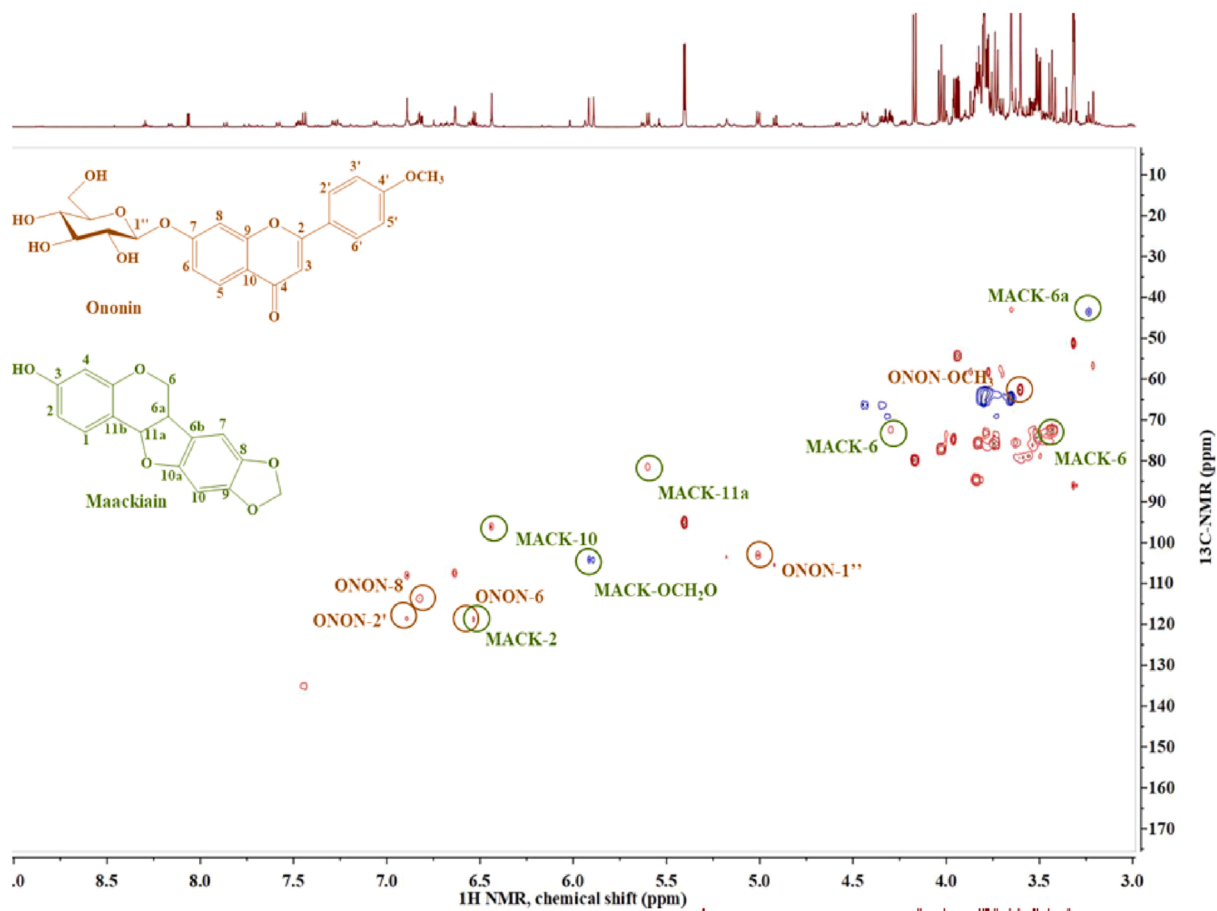
NMR-based metabolite profiling has been well established as a comprehensive platform for phytochemical characterization of complex plant extracts and identification of targeted molecules by using 1- and 2-D NMR spectra. NMR-profiling has broad range of applications, from holistic medicine (distinguishing the eventual therapeutic agents in herbs) up to the comprehensive assessment of pharmacologically active molecules and generation of biomarkers corresponding to the quality and activity of plant-based pharmaceuticals. In the current study, 1- and 2-D NMR-based profiling of 50% aqueous methanol extract from the roots of *O. spinosa* (OSR) has been performed. The most intensive signals in the aromatic region were correlated with the chemical structures of several isoflavones, incl. ononin, sativanone, onogenin, a pterocarpan – maackiain, and spinonin. On the other hand, the presence of several sugars, amino and organic acids was also confirmed (Table S2).

Maackiain and ononin are reported to be among the major metabolites in *O. spinosa*, while other secondary metabolites, e.g. onogenin, sativanone and spinonin, are found in lower amounts [21,29,30]. It has been reported that formononetin, an aglycone of ONON possess anti-adipogenic activity [31], as well as medicarpin [32] – another natural pterocarpan that shares structural similarity to MACK. Therefore, our investigation has focused on ONON and MACK, as potential major contributors of the *O. spinosa* extract activity, which anti-adipogenic activity has not been investigated to the best of our knowledge.

The structure of ONON was identified according to its  $^1\text{H}$  NMR and 2D HSQC spectra (Fig. 1A). In the  $^1\text{H}$  NMR spectrum the three protons H-5, H-6 and H-8 of the ring A represented an ABX spin system. The signal of H-5 showed a coupling constant  $J = 8.7$  Hz ( $\delta_{\text{H}} 7.38/\delta_{\text{C}} 131.26$ ) which confirmed the ortho coupling to H-6  $J = 8.3$ ; 2.3 Hz ( $\delta_{\text{H}} 6.55/\delta_{\text{C}} 114.87$ ). The signal of H-6 exhibited besides the ortho also the meta coupling to H-8 with  $J = 2.5$  Hz ( $\delta_{\text{H}} 6.84/\delta_{\text{C}} 110.37$ ). Along with that the H-5 and H-6 protons were also coupled in the  $^1\text{H}$ - $^1\text{H}$  homonuclear correlation spectroscopy ( $^1\text{H}$ - $^1\text{H}$  COSY) as indicated on Fig. 1B. The two signals at  $\delta_{\text{H}} 6.96/\delta_{\text{C}} 114.92$  ( $J = 8.0$ ; 2.7) and  $\delta_{\text{H}} 6.82/\delta_{\text{C}} 110.74$  ( $J = 8.6$ ; 2.5) characterized the B ring system of the aromatic protons H-2'/H-3' and H-5'/H-6'. Additionally, the B-ring structure was confirmed by the coupling of these protons in the  $^1\text{H}$ - $^1\text{H}$  COSY spectrum. The signals of the  $-\text{OCH}_3$  group were detected at  $\delta_{\text{H}} 3.60/\delta_{\text{C}} 63.38$  (s). The coupling constants of the anomeric proton signal H-1'',  $J = 7.3$  Hz ( $\delta_{\text{H}} 5.01/\delta_{\text{C}} 99.81$ ) proved the presence of  $\beta$ -glucopyranose [33].

The presence of MACK was confirmed according to a set of peaks

A



B

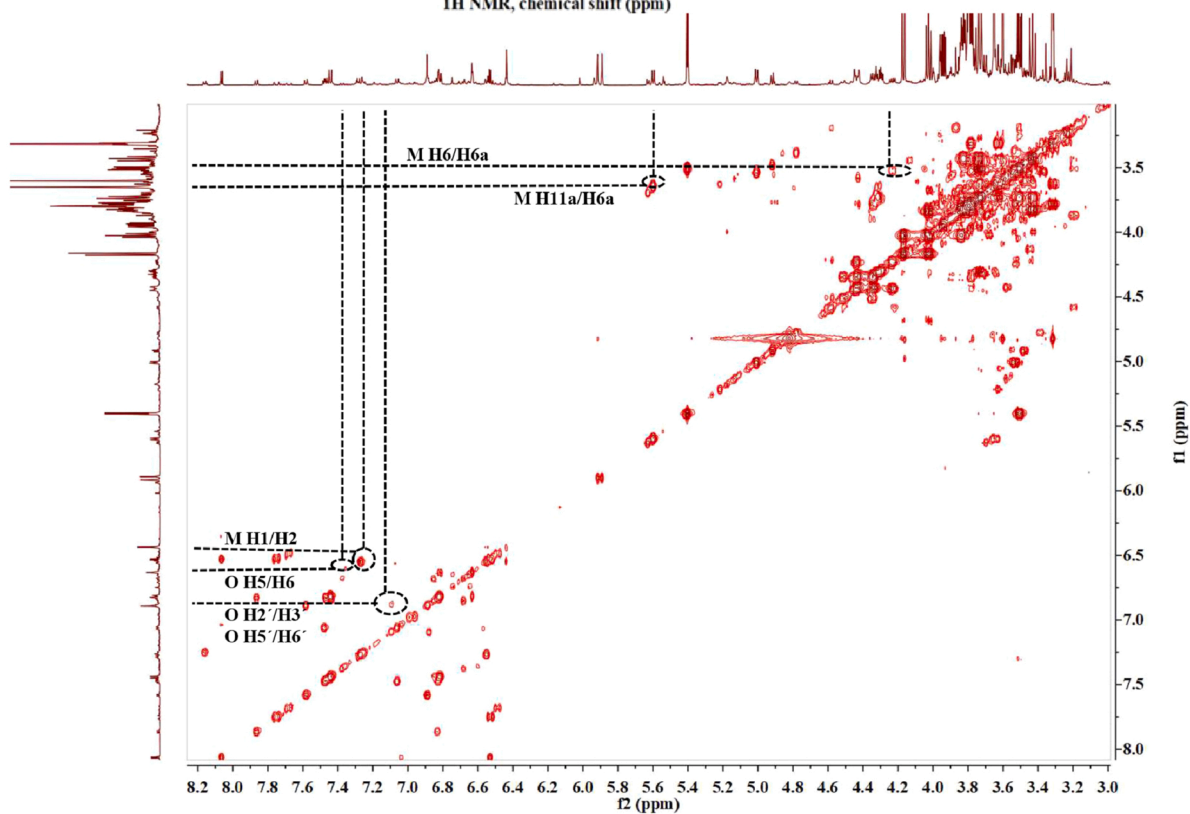


Fig. 1. Heteronuclear single quantum coherence spectroscopy ( $^1\text{H}$ - $^{13}\text{C}$  HSQC, A) and  $^1\text{H}$ - $^1\text{H}$  homonuclear correlation spectroscopy ( $^1\text{H}$ - $^1\text{H}$  COSY, B) spectra of 50% aqueous methanol extract of *Ononis spinosa* L. and characteristic signals of ononin (ONON) and maackiain (MACK).

corresponding to a pterocarpan skeleton in HSQC spectra (Fig. 1A), i.e., the signals as  $\delta_H$  5.60/ $\delta_C$  80.50 ( $J = 7.4$  Hz),  $\delta_H$  4.23/ $\delta_C$  72.89 (m),  $\delta_H$  3.55/ $\delta_C$  72.89 (t,  $J = 10.7$ ) and  $\delta_H$  3.23/ $\delta_C$  43.23 (m) were assigned to H-11a, H-6, H-6 and H-6a, respectively. The spectra also contained the double doublet at  $\delta_H$  5.90/ $\delta_C$  104.31 ( $J = 15.5$ ; 1.0 Hz) corresponding to  $-OCH_2O$  and one singlet at  $\delta_H$  6.42/ $\delta_C$  96.22 (s) and  $\delta_H$  7.26/ $\delta_C$  113.25, corresponding to H-10 and H-8, respectively, suggesting a methylenedioxy moiety of the aromatic D ring. Further, a doublet was identified at  $\delta_H$  6.29/ $\delta_C$  104.5 ( $J = 2.5$  Hz; H-4), a double of doublets at  $\delta_H$  6.55/ $\delta_C$  111.4 ( $J = 8.4$ ; 2.3 Hz) and a doublet at  $\delta_H$  7.27/ $\delta_C$  124.56 ( $J = 8.4$ ; H-1), assigned to the ABX system of the resorcinol nature of the A ring [34,35]. Further, cross-peaks between H-1 and H-2 in the COSY spectrum were also confirmed. Additionally, the COSY spectrum revealed cross-peak between H11a and H6a, which further showed correlation with H6 (Fig. 1B).

### 3.2. In silico molecular docking

Docking runs were conducted to predict the putative affinities of ONON and MACK towards C/EBP $\alpha$ , PPAR $\gamma$ , AMPK, AKT and PI3K. The detailed results are reported in Table 1 and Fig. 2, where putative affinities and non-bond interactions are showed, respectively.

Both ONON and MACK were predicted to interact with the above-mentioned proteins through hydrogen and pi interactions. With the sole exception of MACK towards C/EBP $\alpha$ , both compounds showed good putative affinities, in the submicromolar-micromolar range (0.3–14.7  $\mu$ M). An *in vitro* model constituted by human adipocytes was employed for confirming the results of the prediction and considering concentration ranges of ONON and MACK consistent with their putative affinities towards C/EBP $\alpha$ , PPAR $\gamma$ , AMPK, AKT and PI3K.

### 3.3. O. spinosa root extract, ONON and MACK affected lipid accumulation and decreased basal lipolysis in human adipocytes

Adipose tissue complexity defines its diverse functions: as an energy depot, for maintenance of thermal homeostasis, mechanical support of visceral organs, hormonal regulation, etc. Despite the multicellular character of the fat tissue, adipocytes and their precursors (pre-adipocytes) are the main cells responsible for storage of excess nutrients in the form of triglycerides in lipid droplets [10,36].

Lipid staining of adipocytes, differentiated in the presence of OSR (5, 10 and 25  $\mu$ g/mL), ONON (5, 10 and 25  $\mu$ M) or MACK (5, 10, 25 and 50  $\mu$ M) was performed for evaluation of the lipid accumulation. Representative pictures of stained adipocytes (Fig. 3A) as well as quantification of the results (Fig. 3B) demonstrated modulation of adipogenesis upon all treatments. Significant increase in lipid accumulation to 123.25%, 113.6% and 113.29% for OSR in 5, 10 and 25  $\mu$ g/mL respectively. In contrast to the effect induced by the extract, ONON decreased lipid accumulation significantly as follows 74.3%, 77.85% and 77.63% for 5, 10 and 25  $\mu$ M. Similarly, but to a higher extent, MACK decreased lipid accumulation in concentration-dependent manner: 70.46%, 74.09%, 62.70% and 54.52% correspondingly for 5, 10, 25 and

**Table 1**

Estimated through docking simulation free energy of binding ( $\Delta_G$ , kcal/M) and affinity constant ( $K_i$ ,  $\mu$ M) for ononin and maackiain to proteins of interest, namely peroxisome proliferator-activated receptor gamma (PPAR $\gamma$ ), phosphoinositide 3-kinase (PI3K), adenosine monophosphate-activated protein kinase (AMPK), protein kinase B (AKT) and CCAAT-enhancer-binding protein alpha (CEBP $\alpha$ ) and their protein data bank (PDB) IDs.

Target protein	PDB ID	Ononin	Maackiain
C/EBP $\alpha$	1NWQ	-6.6 kcal/M; 14.7 $\mu$ M	-5.7 kcal/M; 67.2 $\mu$ M
PPAR $\gamma$	2P4Y	-7.9 kcal/M; 1.6 $\mu$ M	-7.9 kcal/M; 1.6 $\mu$ M
AMPK	4CFF	-9.9 kcal/M; 0.06 $\mu$ M	-8.8 kcal/M; 0.4 $\mu$ M
AKT	1O6L	-7.4 kcal/M; 3.8 $\mu$ M	-7.8 kcal/M; 1.9 $\mu$ M
PI3K	5ITD	-9.0 kcal/M; 0.3 $\mu$ M	-8.6 kcal/M; 0.5 $\mu$ M

50  $\mu$ M.

Hydrolysis of triglycerides results in release of free fatty acids and glycerol. Recent investigations hypothesized that increased adipolysis and free-fatty acids plasma levels during obesity aggravate hyperinsulinemia and insulin resistance [37]. Considering free glycerol as a product of adipolysis, measurement of its concentration in the culture media was used as indicator of basal lipolysis. The plant extract and its selected pure compounds significantly decreased glycerol release (Fig. 3C). Mild but significant reduction in released glycerol upon OSR was observed (8.43  $\mu$ M, 6.53  $\mu$ M and 6.73  $\mu$ M at 5, 10 and 25  $\mu$ g/mL, respectively). Similarly, lipolysis was negatively regulated in a concentration-dependent manner by ONON and MACK as the highest decrease was detected by ONON 25  $\mu$ M (4.84  $\mu$ M) and MACK 50  $\mu$ M (5.87  $\mu$ M). Decrease of lipolysis could contribute to the beneficial effect of the tested compounds in the context of improvement of the metabolic dysregulation during obesity.

Collectively, adipogenesis was significantly inhibited by ONON and MACK, and moderately stimulated upon OSR treatment. Notable inhibition of adipolysis was observed in all treatments with the highest inhibitory effect in ONON 25  $\mu$ M.

### 3.4. O. spinosa root extract, ONON and MACK modulated the gene expression of essential adipogenic transcription factors

Selected plant secondary metabolites, namely ONON and MACK, effectively altered the adipogenic and lipolytic capacity of adipocytes. To further elucidate the underlying pathways affected, the relative mRNA expression of key factors related to the initiation of adipogenic differentiation were analysed on day 3 (Fig. S3) and selected adipogenic and lipogenic genes, namely ACC, ADIPOQ, AKT, SERBP1, CEBPA, PI3KCA, PPARG, SIRT1, AMPK, were detected on the 9th day of differentiation (Fig. 4).

To verify if the early stage of adipogenic differentiation is affected, we have investigated the relative gene expression of CEBPB and CEBPD as early differentiation markers [15,38–41] on the 3rd day of differentiation in adipocytes treated with the highest experimental concentrations. Applied treatments significantly downregulated CEBPB and upregulated CEBPD in comparison to the vehicle group (Fig. S3). These results suggest that OSR and its secondary metabolites ONON and MACK interfere within the regulation of adipogenic differentiation in its initiation phase.

The RT-qPCR analysis revealed that OSR significantly downregulated mRNA expression of the gene encoding adiponectin (ADIPOQ, OSR 25  $\mu$ g/mL) and SERBP1 (OSR 5  $\mu$ g/mL). Treatment with MACK in 50  $\mu$ M remarkably inhibited expression of ADIPOQ, ACC, SERBP1, CEBPA, AKT and upregulated AMPK. Increased AKT expression was demonstrated by ONON 10  $\mu$ M. The levels of PI3KCA, SIRT1, AMPK, ACC gene expression were enhanced significantly in the groups treated with ONON 10 and 25  $\mu$ M.

Direct crosstalk between SIRT1 and AMPK is strongly associated with regulation of lipid metabolism. For instance, SIRT1 stimulates AMPK phosphorylation and further inhibition of adipogenesis and lipogenesis by downregulation of lipogenic genes [17,18]. The present study revealed that ONON 10, 25  $\mu$ M and MACK 5, 10, 25, 50  $\mu$ M increased AMPK gene expression in SGBS adipocytes. Furthermore, we analysed the mRNA expression of SIRT1 to assess whether the anti-obesity effect of ONON and MACK is mediated by its modulation.

We propose that ONON 10, 25  $\mu$ M and MACK 5  $\mu$ M decrease lipid accumulation by increase in mRNA expression of the SIRT1 and AMPK. Moreover, the strong anti-adipogenic effect of MACK 50  $\mu$ M was accompanied with suppressed gene expression of major transcription factors such as SERBP1, ACC and CEBPA.

Collectively the data from the gene expression analysis pointed out that MACK and ONON alerted numerous transcription factors from both the early and terminal phases of adipogenic differentiation.

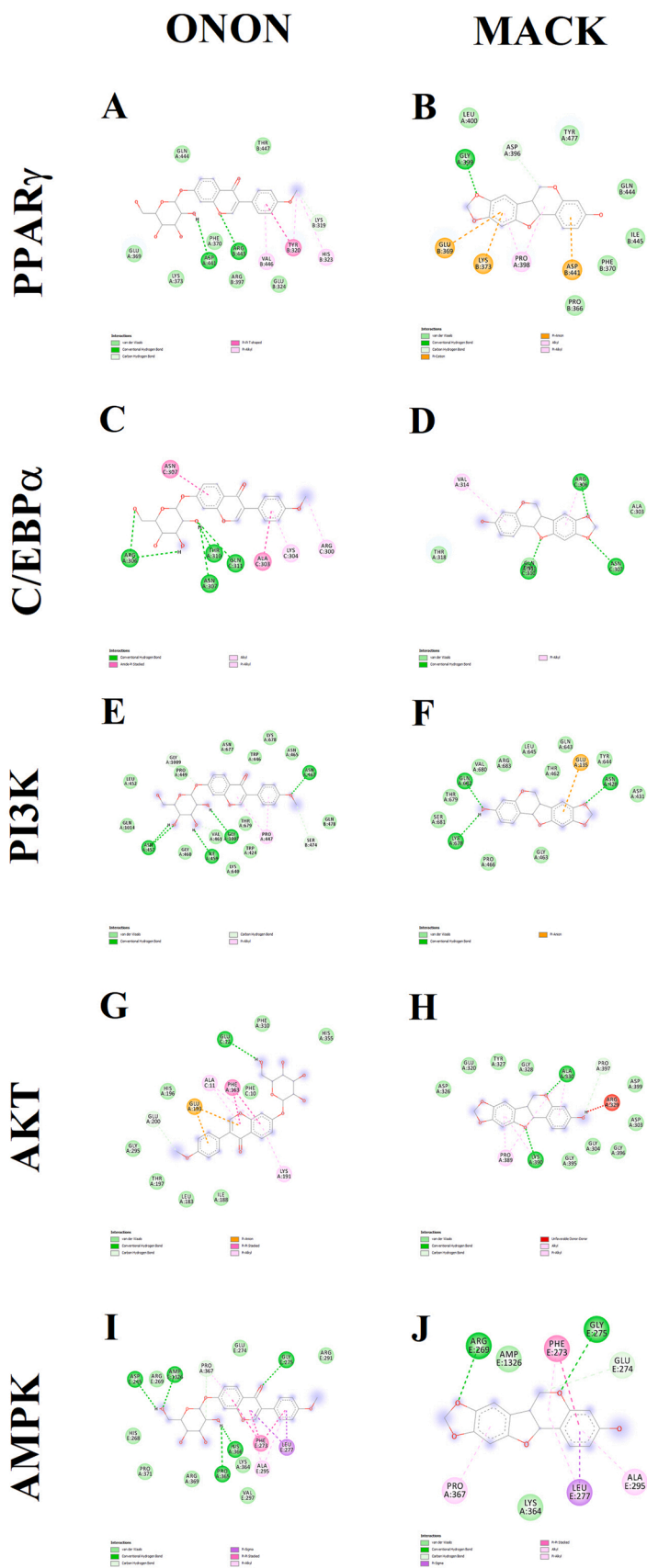


**Fig. 2.** Ononin (ONON) and maackiain (MACK) were indicated to bind with strong affinity towards peroxisome proliferator-activated receptor gamma (PPAR $\gamma$ ), phosphoinositide 3-kinase (PI3K), adenosine monophosphate-activated protein kinase (AMPK), protein kinase B (AKT). Simulated interactions between: ononin and PPAR $\gamma$  (A), ononin and CCAAT-enhancer-binding protein alpha (CEBP $\alpha$ ) (C); ononin and PI3K (E) ononin and AKT (G); ononin and AMPK (I), maackiain and PPAR $\gamma$  (B), maackiain and CEBP $\alpha$  (D); maackiain and PI3K (F); maackiain and AKT (H); maackiain and AMPK (J).

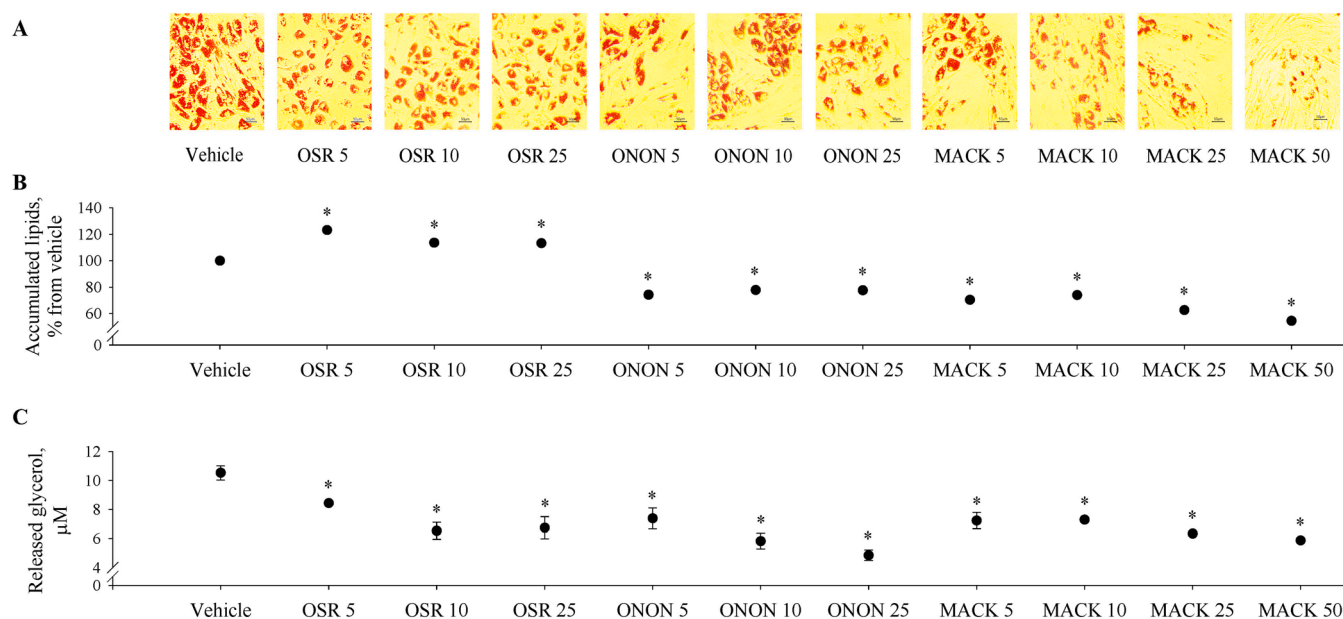


**Fig. 3.** Ononin (ONON) and maackiain (MACK) inhibited adipogenesis, while *Ononis spinosa* L. root extract (OSR) stimulated lipid accumulation during adipocyte differentiation of SGBS human preadipocytes. Representative microphotographs of Oil red O-stained adipocytes on day 9 of differentiation are captured at  $20\times$  magnification, scale bar  $50\ \mu\text{M}$  (A). Quantification of lipid staining as percentage from differentiated vehicle-treated control group after isopropanol extraction (B). Concentration of released glycerol ( $\mu\text{M}$ ) as an index of basal lipolysis after incubation for 24 h with OSR, ONON or MACK (C). The experimental data are shown as mean  $\pm$  SEM, from three independent experiments. Significant differences were assigned to  $*p < 0.05$  compared with the vehicle.

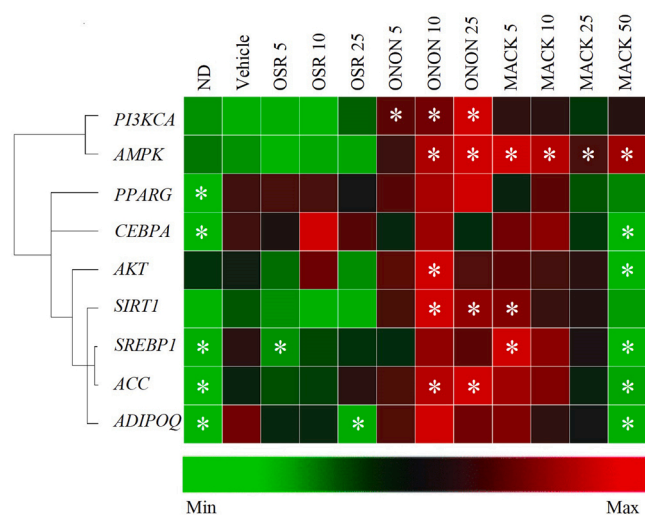


**Fig. 4.** Clustergram and heatmap of the relative gene expression on the 9th day of differentiation performed by RT-qPCR analysis. The data are representative of three independent experiments (mean  $\pm$  SEM),  $*p < 0.05$  compared to vehicle group. mRNA expression values of target genes were normalized to *RPL13A* and *TUBB*.

### 3.5. Protein abundance of key adipogenic transcription factors is affected upon treatment with ONON and MACK

Adipocyte differentiation is a complex and precisely regulated process, triggered by different stimuli, which early phase is coordinated by C/EBP $\beta$  and  $\delta$ , while the terminal phase is hence directed by the tandem of two major transcription factors - C/EBP $\alpha$  and PPAR $\gamma$ . Insulin- and insulin-like growth factor 1 (IGF-1)-triggered adipogenesis is mediated by the PI3K/AKT signaling pathway [38]. The metabolic function of AMPK upon phosphorylation is related to inhibition of adipogenic markers and simultaneously intensification of fatty acid oxidation [39]. Modulation of this mechanism is a promising approach for identifying

potential compounds with anti-adipogenic activity. To reinforce the data from the RT-qPCR analysis, the protein abundance analysis of several major regulators of adipogenesis was measured (PPAR $\gamma$ , AKT, AMPK, pAMPK, adiponectin, C/EBP $\alpha$ , PI3K).

The molecular docking predictions suggested strong probability for interaction between both ONON and MACK and PI3K, PPAR $\gamma$  and AMPK at a protein level. Correspondingly, inhibition of PI3K by ONON 5, 25  $\mu\text{M}$  and MACK 5, 10, 50  $\mu\text{M}$  was observed (Fig. 5D). A reduction in the levels of PPAR $\gamma$  protein was achieved by ONON 25  $\mu\text{M}$ , MACK 5 and 50  $\mu\text{M}$  (Fig. 5C). However, the protein abundance of AMPK (Fig. 5F) and its active form pAMPK (Fig. 5G) were only moderately decreased upon supplementation with ONON 5, 10  $\mu\text{M}$  and MACK 5  $\mu\text{M}$ . In agreement with the RT-qPCR analysis, MACK 50  $\mu\text{M}$  significantly reduced C/EBP $\alpha$  protein abundance (Fig. 5B).

As a marker of adipocyte maturation [40], adiponectin levels are significantly and concentration-dependently decreased by the treatment of OSR at 25  $\mu\text{g}/\text{mL}$  as well as with ONON and MACK in the whole range of the applied concentration (Fig. 5A). Despite the confirmed inhibition of adipocyte differentiation, the levels of adiponectin should be strictly monitored because its levels are reported to be correlated with insulin sensitivity [40].

Maackiain at its highest concentration applied (50  $\mu\text{M}$ ) significantly downregulated the protein expression of the key regulators of adipogenesis - PPAR $\gamma$  and C/EBP $\alpha$ . The results of the protein analysis supported the suggestion that MACK inhibited adipogenesis through the PPAR $\gamma$ /C/EBP $\alpha$  pathway.

### 3.6. Proposed anti-adipogenic mechanism of *O. spinosa* root extract, ONON and MACK

Adipogenesis is a tightly regulated process, which could be affected by modulation of signaling molecules engaged in the adipogenic cascade (Fig. 6).

Adipocyte differentiation is induced by stimuli such as insulin and IGF-1. Further, insulin signaling is mediated via activation of the PI3K/AKT and the RAS/mitogen-activated protein kinase (MAPK) pathway [38]. Once triggered, adipogenesis is governed by a short-term

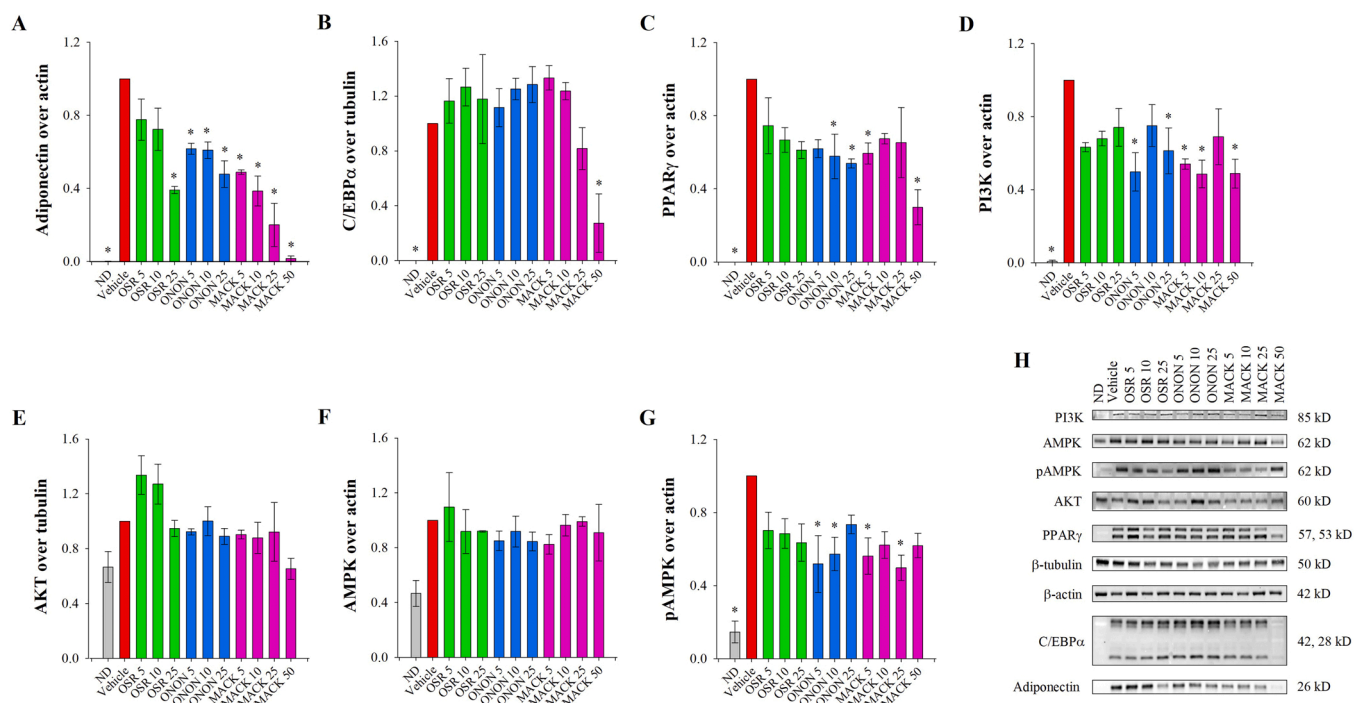


**Fig. 5.** Protein level of adiponectin (A), CCAAT-enhancer-binding protein alpha (C/EBPα; B), peroxisome proliferator-activated receptor gamma (PPARγ; C), phosphoinositide 3-kinase (PI3K; D), protein kinase B (AKT; E), adenosine monophosphate-activated protein kinase (AMPK; F), phosphorylated AMPK (pAMPK; G), normalized to β-actin or β-tubulin. Representative images of the Western blots (H). Results are obtained from three independent experiments, expressed as mean ± SEM, \*p < 0.05 compared to vehicle group.

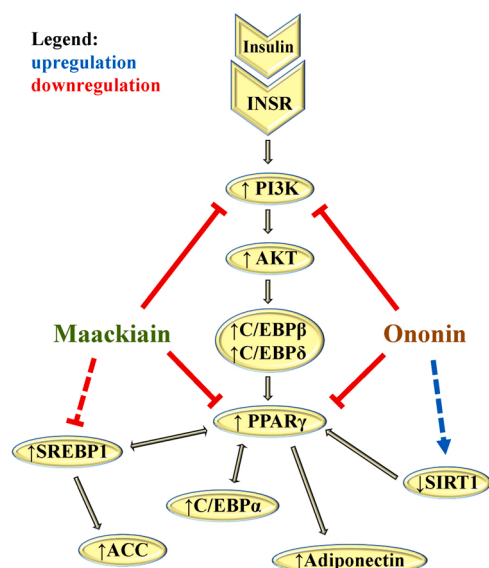


**Fig. 6.** Adipogenic cascade and proposed mechanisms of anti-adipogenic and/or anti-lipogenic effects of ononin (ONON) and maackiain (MACK) identified in *Ononis spinosa* L. root extract. Both ONON and MACK inhibited phosphoinositide 3-kinase (PI3K) as mediator of insulin signaling through insulin receptor (INSR) induction of differentiation that subsequently resulted in changes in CCAAT-enhancer-binding protein beta (C/EBPβ) and δ mRNA expression. In addition, ONON activated sirtuin-1 (SIRT1) which is a negative regulator of the most important transcription factor for terminal adipogenic differentiation peroxisome proliferator-activated receptor gamma (PPARγ) and also inhibited the late adipogenic marker - adiponectin. MACK mitigated adipogenesis via suppression of PPARγ and C/EBPα signaling as well as adiponectin with subsequent decrease in lipogenesis mediated by sterol regulatory element-binding protein 1 (SREBP1) and its downstream target acetyl-CoA carboxylase (ACC).

expression of C/EBPβ and δ during the early adipogenic phase, followed by characteristic upregulation of PPARγ and C/EBPα to terminate adipocyte differentiation and induce lipogenesis [41]. An important lipogenic transcription factor is SREBP1 and its target genes ACC and FAS encoding key enzymes in lipid biogenesis [42]. The current investigation revealed that the pure secondary metabolites of OSR, namely ONON and MACK inhibited the process of adipogenic differentiation of human adipocytes. The obtained results suggest moderate influence on the early molecular regulation of adipogenic differentiation upon OSR treatment. Despite the moderate increase in accumulated lipids that was observed on the Oil red O assay, neither the gene expression profile nor the protein abundance of the evaluated late adipogenic markers were significantly affected by the application of the OSR extract except for that of adiponectin from OSR 25 μg/mL.

Direct molecular interaction between PI3K and PPARγ and both pure compounds was predicted with strong affinity by the docking calculations and further confirmed from the Western blot results. We could speculate that the suppression of ONON and MACK on PI3K results in alternations within the mRNA expression levels of the early adipogenic markers C/EBPβ and δ. The pure secondary metabolite MACK strongly inhibited adipogenesis and lipogenesis by decreasing of SREBP1, ACC gene expression. Additionally, MACK induced reduction in the protein abundance of PI3K as a mediator in the initiation of adipogenic transformation and diminished the protein expression of late adipogenic-specific transcription factors such as PPARγ, C/EBPα and adiponectin in human adipocytes. In a similar manner, ONON exhibited its anti-adipogenic effect through decreased PI3K protein abundance, increased expression of SIRT1, followed by inhibition of PPARγ and adiponectin.

Collectively, both secondary metabolites (ONON and MACK) inhibited PI3K - suggesting interaction of the pure compounds within the early stages of adipogenic differentiation. MACK inhibited adipogenesis through PPARγ/C/EBPα signaling and decreased lipogenesis by downregulation of SREBP1 and its downstream lipogenic genes. On the other hand, ONON exhibits solely an anti-adipogenic effect via



upregulation of SIRT1 and inhibition of PPAR $\gamma$ . Furthermore, ONON and MACK decreased adiponectin levels, which could be eventually a secondary effect to the PPAR $\gamma$  modulation.

#### 4. Discussion

Obesity is a multifactorial disease that impairs the quality of life and reduces the life span of the patients. Increased mass of adipose tissue in obesity results from both hyperplasia and hypertrophy of adipocytes. Inhibition of the adipocyte differentiation and modulation of lipolysis are possible molecular mechanisms in treatment of obesity and its related complications [8]. Terminal adipocyte differentiation is governed by PPAR $\gamma$  and C/EBP $\alpha$ , while SREBP1 is responsible for the control of lipogenesis. In addition, the transcriptional activity of PPAR $\gamma$ , along with adipogenesis could be negatively influenced by activation of SIRT1. Moreover, successful reduction of the excess adipose tissue expansion is observed upon inhibition of the PI3K/AKT signaling pathway [9,11–14] which reveal another target for obesity treatment.

Natural products are utilized as a potential source of novel bioactive leads for obesity management and are assumed to be safer than conventional pharmacotherapy [6]. In this context, plant extracts could provide various secondary metabolites that can alleviate the abnormal expansion and the dysfunction of the adipose tissue and so to improve the anti-obesity therapeutic options.

The extract of *O. spinosa* roots is abundant in different classes of secondary metabolites [21,23,43]. Based on the ethnopharmacological use of OSR extract for treatment of metabolic disturbances, including obesity, and the lack of scientific evidence related to the effect of OSR on adipogenesis, we have investigated for the first time the anti-adipogenic potential of OSR in an *in vitro* obesity model of human adipocytes. Analysis of the OSR proton NMR spectra revealed the presence of ononin, sativanone, onogenin, spinonin and maackiain as secondary metabolites, which was in accordance with the literature data [22,23]. Additional analysis of the 2D NMR spectra of the plant extract confirmed the presence of ONON and MACK as secondary metabolites which were selected for further biological experiments along with the OSR.

Interestingly, OSR significantly stimulated adipogenesis assessed by lipid staining, and decreased lipid hydrolysis, measured by released in the culture media glycerol. Moreover, results from analysis of relative mRNA and protein expression indicated moderate decrease of adiponectin by OSR only in the highest concentration applied. These findings propose that OSR does not directly target the molecular regulatory pathways of adipogenic differentiation tested in our investigation. Its apparent effect in improvement of metabolic impairments could rather involve other molecular pathways or organs and tissues different from the adipose depot which requires to be clarified in *in vivo* settings. However, both ONON and MACK provoked a reduction in the differentiation rates of human adipocytes which highlights the importance of OSR as a source of natural bioactive anti-obesity compounds.

The isoflavone glycoside ONON is reported within numerous plants such as *Smilax scobinicaulis* C.H. Wright, *Millettia nitida* Benth. and *Ononis* species [22,23,43–47]. Despite the scarce literature data regarding its biological activity, anti-inflammatory, anti-angiogenic and antiviral potential have been suggested [44–47]. A decrease in inflammatory response upon treatment with ONON is described in lipopolysaccharide-stimulated RAW 264.7 macrophages [44], which reveals the therapeutic potential of this metabolite in inflammation-related pathologies. A recent investigation reported that ONON exhibited a neuroprotective effect in a murine model of Alzheimer's disease by modulation of brain-derived neurotrophic factor, PPAR $\gamma$ , p38 MAPK, and nuclear factor kappa-light-chain-enhancer of activated B cells (NF- $\kappa$ B)/p65 levels in brain tissue [47]. Even though ONON is not investigated for anti-adipogenic effect so far, its aglycone part - formononetin - was reported to inhibit adipogenesis through the AMPK/ $\beta$ -catenin signalling pathway *in vivo* in diet-induced obesity murine model [31]. Similarly, in our study, the adipocyte differentiation

along with lipolysis were markedly decreased in the presence of ONON. The *in silico* docking prediction suggested possible interactions between ONON and the investigated protein targets - AMPK, PI3K, PPAR $\gamma$ , C/EBP $\alpha$  and AKT. However, an actual reduction in the protein abundance was detected for PI3K and PPAR $\gamma$  by Western blotting as a result of ONON treatment. The suppression of PI3K by ONON could be the trigger of the alterations on the early phase transcription factors C/EBP $\beta$  and  $\delta$ . Regarding the AMPK protein level our results are consistent with that of Gautam et al. [31] as their study reports absence of any change in AMPK total protein level during nine days of differentiation in murine 3T3-L1 adipocytes. However, in contrast to this report, we do not detect an increase in AMPK phosphorylation. One possible explanation is that formononetin could have greater affinity towards AMPK than ONON. Another could be that, in human adipocytes, the time-dependent activation of pAMPK occurs before day nine, hence it remains undetected in the current experimental set up. Upregulation of SIRT1 is known to protect from metabolic impairments through interplay with PPAR $\gamma$  [19] and/or AMPK [17,18,48,49]. Moreover, SIRT1 upregulation is correlated with decreased adipogenesis along with enhanced osteogenesis [48]. Our findings support that ONON upregulated *SIRT1* independently of AMPK activation which could be crucial for the observed anti-adipogenic effect of ONON. Altogether, the anti-adipogenic effect of ONON is likely to be mediated by inhibition of PI3K, upregulation of *SIRT1* followed by decrease in PPAR $\gamma$  and adiponectin levels.

Maackiain is a pterocarpan that has been proposed to possess anti-allergic, anti-cancer, anti-inflammatory and antimicrobial activity, as well as, to inhibit monoamine oxidase B [50–52]. The reported anti-allergic activity of MACK is mediated by suppression of histamine H1 receptor *via* inhibition of protein kinase C- $\delta$  (PKC $\delta$ ) activation through the disruption of heat-shock protein 90 -PKC $\delta$  interaction [51]. In addition, MACK inhibits the differentiation and the bone-resorbing functions of murine osteoclasts *via* suppression of the NF- $\kappa$ B signalling pathway [52]. Considering the mechanistic interconnections between adipogenesis and osteogenesis [53], inhibition of bone resorption by MACK could have common molecular targets with its anti-adipogenic mechanism in adipocytes. Concentration-dependent decrease in lipid accumulation and triglyceride hydrolysis were observed upon MACK treatment in our study. Maackiain modulated the expression of the master adipogenic transcription factors *CEBPA*, *CEBPB*, *CEBPD* and *SERBP1*, and the lipogenic enzyme gene *ACC*. In addition, MACK markedly increased the gene expression of *AMPK*. As indicated from the docking results, a possible interaction between the investigated target proteins and MACK were confirmed *via* Western blot as a notable decrease in PI3K, PPAR $\gamma$ , C/EBP $\alpha$  and adiponectin. Changes in neither the total AMPK nor in the phosphorylated form were detected upon MACK treatment. However, the strong binding affinity suggested by the docking results and the concentration-dependent transcriptional activation of this gene suggests that MACK may warrant further investigation as AMPK modulator. Similar to the suggested explanation on the effect of ONON on AMPK activity, we could speculate that MACK affects the protein phosphorylation at a different time-point during adipogenic transformation in human adipocytes. Moreover, our findings revealed that MACK reduced lipid accumulation by decreasing lipogenesis *via* suppression of *SREBP1* and *ACC*, as well as inhibition of the adipogenic-specific transcription factors PPAR $\gamma$  and C/EBP $\alpha$  in human adipocytes.

Collectively, our results demonstrate that OSR does not hamper adipogenesis while both MACK and ONON decrease lipid accumulation substantially. The suppressive effect of MACK and ONON on lipid accumulation was reported for the first time in human adipocytes. The most probable mechanism of action of ONON is *via* suppression of PI3K, activation of *SIRT1* and subsequent inhibition of the PPAR $\gamma$ /adiponectin axis activity. The potent anti-adipogenic activity of MACK is mediated through modulation of PI3K and the PPAR $\gamma$ /C/EBP $\alpha$  signaling and restriction of lipogenesis by inhibition of *SREBP1* and *ACC*. Both compounds produce substantial anti-adipogenic effect that merits further *in*

vivo validation.

## Funding

This research received funding from the European Union's Horizon 2020 research and innovation programme, project PlantaSYST (SGA No 739582 under FPA No. 664620), and the BG05M2OP001-1.003-001-C01 project, financed by the European Regional Development Fund through the "Science and Education for Smart Growth" Operational Programme.

## CRedit authorship contribution statement

**Saveta G. Mladenova:** Conceptualization, Methodology, Formal analysis, Data curation, Writing – original draft, Visualization, Investigation. **Martina S. Savova:** Conceptualization, Methodology, Formal analysis, Data curation, Writing – original draft, Visualization, Investigation. **Andrey S. Marchev:** Formal analysis, Data curation, Writing – review & editing. **Claudio Ferrante:** Software, Data Curation, Writing – original draft, Visualization. **Giustino Orlando:** Software, Writing – review & editing. **Martin Wabitsch:** Methodology, Writing – review & editing. **Milen I. Georgiev:** Conceptualization, Methodology, Supervision, Funding acquisition, Writing – review & editing.

## Conflict of interest statement

Author Saveta G. Mladenova is employed by BB-NCIPD Ltd., National Center of Infectious and Parasitic Diseases, Ministry of Health. The remaining authors declare that the research was conducted in the absence of any commercial or financial relationships that could be construed as a potential conflict of interest.

## Data availability

Data will be made available on request.

## Acknowledgements

The authors are grateful to Dr. Liliya Mihaylova (Center of Plant Systems Biology and Biotechnology) for her great assistance during the data analysis, review and editing of the manuscript and to Dr. Rafe Lyall (Center of Plant Systems Biology and Biotechnology) for proofreading and editing the manuscript.

## Appendix A. Supporting information

Supplementary data associated with this article can be found in the online version at [doi:10.1016/j.biopha.2022.112908](https://doi.org/10.1016/j.biopha.2022.112908).

## References

- M. Safaei, E. Sundararajan, M. Driss, W. Boulila, A. Shapi, A systematic literature review on obesity: Understanding the causes and consequences of obesity and reviewing various machine learning approaches used to predict obesity, *Comput. Biol. Med.* 136 (2021), 104754.
- L. Vasileva, M. Savova, K. Amirova, Z. Balcheva-Sivenova, C. Ferrante, G. Orlando, M. Wabitsch, M. Georgiev, Caffeic and chlorogenic acids synergistically activate browning program in human adipocytes: Implications of AMPK- and PPAR-mediated pathways, *Int. J. Mol. Sci.* 21 (2020) 9740.
- P. Petrus, T. Fernandez, M. Kwon, J. Huang, V. Lei, N. Safikhani, S. Karunakaran, D. O'Shannessy, X. Zheng, S.-B. Catrina, E. Albone, J. Laine, K. Virtanen, S. Clee, T. Kieffer, C. Noll, A. Carpentier, J. Johnson, M. Rydén, E. Conway, Specific loss of adipocyte CD248 improves metabolic health via reduced white adipose tissue hypoxia, fibrosis and inflammation, *EBioMedicine* 44 (2019) 489–501.
- L. Vasileva, A. Marchev, M. Georgiev, Causes and solutions to "globesity": The new fat(s)t alarming global epidemic, *Food Chem. Toxicol.* 121 (2018) 173–193.
- D. Bessesen, L. Van Gaal, Progress and challenges in anti-obesity pharmacotherapy, *Lancet Diabetes Endocrinol.* 6 (2017) 237–248.
- G. Sandner, A. Konig, M. Wallner, J. Weghuber, Functional foods - dietary or herbal products on obesity: application of selected bioactive compounds to target lipid metabolism, *J. Food Sci.* 34 (2019) 9–20.
- S. Karri, S. Sharma, K. Hatware, K. Patil, Natural anti-obesity agents and their therapeutic role in management of obesity: A future trend perspective, *Biomed. Pharmacother.* 110 (2019) 224–238.
- A. Santos, S. Sinha, Obesity and aging: Molecular mechanisms and therapeutic approaches, *Ageing Res. Rev.* 67 (2021), 101268.
- A. Ortega-Molina, E. Lopez-Guadamillas, R. de Cabo, M. Serrano, Pharmacological inhibition of PI3K reduces adiposity and metabolic syndrome in obese mice and rhesus monkeys, *Cell Metab.* 21 (2015) 558–570.
- A.G. Cristancho, M.A. Lazar, Forming functional fat: a growing understanding of adipocyte differentiation, *Nat. Rev. Mol. Cell Biol.* 12 (2011) 722–734.
- E. Lopez-Guadamillas, M. Munoz-Martin, S. Martinez, J. Pastor, P.J. Fernandez-Marcos, M. Serrano, PI3K $\alpha$  inhibition reduces obesity in mice, *Aging* 8 (2016) 2747–2753.
- L.C. Foukas, B. Bilanges, L. Bettedi, W. Pearce, K. Ali, S. Sancho, D.J. Withers, B. Vanhaesebroeck, Long-term p110 $\alpha$  PI3K inactivation exerts a beneficial effect on metabolism, *EMBO Mol. Med.* 5 (2013) 563–571.
- E. Jeffery, C.D. Church, B. Holtrup, L. Colman, M.S. Rodeheffer, Rapid depot-specific activation of adipocyte precursor cells at the onset of obesity, *Nat. Cell Biol.* 17 (2015) 376–385.
- S. Nagai, C. Matsumoto, M. Shibano, K. Fujimori, Suppression of fatty acid and triglyceride synthesis by the flavonoid orientin through decrease of C/EBP $\delta$  expression and inhibition of PI3K/Akt-FOXO1 signaling in adipocytes, *Nutrients* 10 (2018) 130.
- Y. Choi, J. Shim, M. Kim, M. Genistin: a novel potent anti-adipogenic and anti-lipogenic agent, *Molecules* 25 (2020) 2042.
- J. Je, J. Park, Y. Seo, J. Han, HM-chromanone inhibits adipogenesis by regulating adipogenic transcription factors and AMPK in 3T3-L1 adipocytes, *Eur. J. Pharmacol.* 892 (2021), 173689.
- H. Lee, S.-M. Lim, J. Jung, S. Kim, J. Lee, Y. Kim, K. Cha, T. Oh, J. Moon, T. Kim, E. Kim, *Gynostemma pentaphyllum* extract ameliorates high-fat diet-induced obesity in C57BL/6N mice by upregulating SIRT1, *Nutrients* 11 (2019) 2475.
- C.-J. Liou, S.-J. Wu, S.-C. Shen, L.-C. Chen, Y.-L. Chen, W.-C. Huang, Phloretin ameliorates hepatic steatosis through regulation of lipogenesis and Sirt1/AMPK signaling in obese mice, *Cell Biosci.* 10 (2020) 114.
- S. Perrini, S. Porro, P. Nigro, A. Cignarelli, C. Caccioppoli, V.A. Genchi, G. Martines, M. De Fazio, P. Capuano, A. Natalicchio, L. Laviola, F. Giorgino, Reduced SIRT1 and SIRT2 expression promotes adipogenesis of human visceral adipose stem cells and associates with accumulation of visceral fat in human obesity, *Int. J. Obes.* 44 (2019) 307–319.
- R. Mayoral, O. Osborn, J. McNelis, A.M. Johnson, D.Y. Oh, C.L. Izquierdo, H. Chung, P. Li, P.G. Traves, G. Bandyopadhyay, A.R. Pessentheiner, J.M. Ofrecio, J.R. Cook, L. Qiang, D. Accili, J.M. Olefsky, Adipocyte SIRT1 knockout promotes PPAR $\gamma$  activity, adipogenesis and insulin sensitivity in chronic-HFD and obesity, *Mol. Metab.* 4 (2015) 378–391.
- H. Abdessellem, A. Madani, A. Hani, M. Al-Noubi, N. Goswami, H.B. Hamidane, A. M. Billing, J. Pasquier, M.S. Bonkowski, N. Halabi, R. Dalloul, M.Z. Sherif, N. Mesaali, M. ElRayess, D.A. Sinclair, J. Graumann, N.A. Mazloum, SIRT1 limits adipocyte hyperplasia through c-Myc inhibition, *J. Biol. Chem.* 291 (2016) 2119–2135.
- N. Gampe, A. Darcsi, S. Lohner, S. Béni, L. Kursinszki, Characterization and identification of isoflavonoid glycosides in the root of Spiny retharow (*Ononis spinosa* L.) by HPLC-QTOF-MS, HPLC-MS/MS and NMR, *J. Pharm. Biomed. Anal.* 123 (2016) 74–81.
- N. Addotey, I. Lengers, J. Jose, N. Gampe, S. Béni, F. Petereit, A. Hensel, Isoflavonoids with inhibiting effects on human hyaluronidase-1 and norneolignan clitorienolactone B from *Ononis spinosa* L. root extract, *Fitoterapia* 30 (2018) 169–174.
- E. Öz, S. Bşcan, K. Akkol, I. Süntar, H. Keleş, B. Acıkara, Wound healing and anti-inflammatory activity of some *Ononis* taxons, *Biomed. Pharmacother.* 91 (2017) 1096–1105.
- V. Spiegler, B. Gierlikowska, T. Saenger, L. Addotey, J. Sendker, J. Jose, A. Kiss, H. Andreas, Root extracts from *Ononis spinosa* inhibit IL-8 release via interactions with toll-like receptor 4 and lipopolysaccharide, *Front. Pharmacol.* 11 (2020) 889.
- S. Mladenova, L. Vasileva, M. Savova, A. Marchev, D. Tews, M. Wabitsch, C. Ferrante, G. Orlando, M. Georgiev, Anti-adipogenic effect of *Alchemilla monticola* is mediated via PI3K/AKT signaling inhibition in human adipocytes, *Front. Pharmacol.* 12 (2021), 707507.
- M. Wabitsch, R.E. Brenner, I. Melzner, M. Braun, P. Möller, E. Heinze, K. M. Debatin, H. Hauner, Characterization of a human preadipocyte cell strain with high capacity for adipose differentiation, *Int. J. Obes.* 25 (2001) 8–15.
- L. Vasileva, M. Savova, D. Tews, M. Wabitsch, M. Georgiev, Rosmarinic acid attenuates obesity and obesity-related inflammation in human adipocytes, *Food Chem. Toxicol.* 149 (2021), 112002.
- B. Klejdus, J. Vacek, L. Lojkova, L. Benesova, V. Kunban, Ultrahigh-pressure liquid chromatography of isoflavones and phenolic acids on different stationary phases, *J. Chromatogr. A* 1195 (2008) 52–59.
- N. Gampe, E. Nagy, L. Kursinszki, S. Beni, Quantitative determination of isoflavonoids in *Ononis* species by UPLC-UV-DAD, *Phytochem. Anal.* 31 (2021) 474–481.
- J. Gautam, V. Khedgikar, P. Kushwaha, D. Choudhary, G. Nagar, K. Dev, P. Dixit, D. Singh, R. Maurya, R. Trivedi, Formononetin, an isoflavone, activates AMP-activated protein kinase/ $\beta$ -catenin signalling to inhibit adipogenesis and rescues

- C57BL/6 mice from high-fat diet-induced obesity and bone loss, *Br. J. Nutr.* 117 (2017) 645–661.
- [32] K.M. Imran, D. Yoon, Y.-S. Kim, A pivotal role of AMPK signaling in medicarpin-mediated formation of brown and beige adipocytes from C3H10T1/2 mesenchymal stem cells, *Biofactors* 44 (2018) 168–179.
- [33] M. Bernhardt, H. Shaker, A. Elgamel, K. Seifert, The new bishomoflavone ononin and its glucoside from *Ononis vaginalis*, *J. Biosci.* 55c (2000) 516–519.
- [34] A.J. Park, J.H. Kim, C. Jin, K.-T. Lee, S.Y. Lee, A new pterocarpans, (-)-maackiain sulfate, from the roots of *Sophora subprostrata*, *Arch. Pharm. Res.* 12 (2003) 1009–1013.
- [35] Z. Wu, Y.-Z. Cai, R. Yuan, Q. Wan, D. Xiao, J. Lei, J. Yu, Bioactive pterocarpans from *Trigonella foenum-graecum* L., *Food Chem.* 313 (2020), 126092.
- [36] A. Ramirez, S. Dankel, B. Rastegarpanah, W. Cai, R. Xue, M. Crovella, Y.-H. Tseng, C. Kahn, S. Kasif, Single-cell transcriptional networks in differentiating preadipocytes suggest drivers associated with tissue heterogeneity, *Nat. Commun.* 11 (2020) 2117.
- [37] E. Fryk, J. Olausson, K. Mossberg, L. Strindberg, M. Schmelz, H. Brogren, L.-M. Gan, S. Piazza, A. Provenzano, B. Becattini, L. Lind, G. Solinas, P.-A. Jansson, Hyperinsulinemia and insulin resistance in the obese may develop as part of a homeostatic response to elevated free fatty acids: A mechanistic case-control and a population-based cohort study, *EBioMedicine* 65 (2021), 103264.
- [38] M. Mandl, S. Wagner, F. Hatzmann, M. Mitterberger-Vogt, M. Zwierzina, M. Mattesich, W. Zwerschke, Sprout1 is a weight-loss target gene in human adipose stem/progenitor cells that is mandatory for the initiation of adipogenesis, *Cell Death Dis.* 10 (2019) 411.
- [39] M. Jo, M. Kim, M. Jo, N. Abid, M. Kim, Adiponectin homolog osmotin, a potential anti-obesity compound, suppresses abdominal fat accumulation in C57BL/6 mice on high-fat diet and in 3T3-L1 adipocytes, *Int. J. Obes.* 43 (2019) 2422–2433.
- [40] D. Mosefi, A. Regassa, W.-K. Kim, Molecular regulation of adipogenesis and potential anti-adipogenic bioactive molecules, *Int. J. Mol. Sci.* 17 (2016) 124.
- [41] P. Tang, S. Virtue, J.Y.G. Goie, C.W. Png, J. Guo, Y. Li, H. Jiao, Y.L. Chua, M. Campbell, J.M. Moreno-Navarrete, A. Shabbir, J.-M. Fernández-Real, S. Gasser, D.M. Kemeny, H. Yang, A. Vidal-Puig, Y. Zhang, Regulation of adipogenic differentiation and adipose tissue inflammation by interferon regulatory factor 3, *Cell Death Differ.* 28 (2021) 3022–3035.
- [42] R. Bertolio, F. Napoletano, M. Mano, S. Maurer-Stroh, M. Fantuz, A. Zannini, S. Bicchato, G. Sorrentino, G. Del Sal, Sterol regulatory element binding protein 1 couples mechanical cues and lipid metabolism, *Nat. Commun.* 10 (2019) 1326.
- [43] N. Gampe, A. Darcsi, L. Kursinszki, S. Béni, Separation and characterization of homopipercolic acid isoflavonoid ester derivatives isolated from *Ononis spinosa* L. root, *J. Chromatogr. B* 1091 (2018) 21–28.
- [44] L. Dong, L. Yin, Y. Zhang, X. Fu, J. Lu, Anti-inflammatory effects of ononin on lipopolysaccharide-stimulated RAW 264.7 cells, *Mol. Immunol.* 83 (2017) 46–51.
- [45] Y. Yu, Z. Li, R. Guo, J. Qian, H. Zhang, J. Zhang, X. Zhao, S. Wang, Y. Wang, Ononin, sec-O-β-D-glucosylhamaudol and astragaloside I: antiviral lead compounds identified via high throughput screening and biological validation from traditional Chinese medicine Zhongjing formulary, *Pharmacol. Res.* 145 (2019), 104248.
- [46] G. Gong, Y. Zheng, X. Kong, Z. Wen, Anti-angiogenesis function of ononin via suppressing the MEK/Erk signaling pathway, *J. Nat. Prod.* 84 (2021) 1755–1762.
- [47] X. Chen, M. Zhang, M. Ahmed, K. Surapaneni, V. Veeraraghavan, P. Arulselvan, Neuroprotective effects of ononin against the aluminium chloride-induced Alzheimer's disease in rats, *Saudi J. Biol. Sci.* 28 (2021) 4232–4239.
- [48] J. Song, J. Li, F. Yang, G. Ning, L. Zhen, L. Wu, Y. Zheng, Q. Zhang, D. Lin, C. Xie, L. Peng, Nicotinamide mononucleotide promotes osteogenesis and reduces adipogenesis by regulating mesenchymal stromal cells via the SIRT1 pathway in aged bone marrow, *Cell Death Dis.* 10 (2019) 336.
- [49] H. Yao, X. Tao, L. Xu, Y. Qi, L. Yin, X. Han, Y. Xu, L. Zheng, J. Peng, Dioscin alleviates non-alcoholic fatty liver disease through adjusting lipid metabolism via SIRT1/AMPK signaling pathway, *Pharmacol. Res.* 131 (2018) 51–60.
- [50] R.-T. Tsai, C.-W. Tsai, S.-P. Liu, J.-X. Gao, Y.-H. Kuo, P.-M. Chao, H.-S. Hung, W.-C. Shyu, S.-Z. Lin, R.-H. Fu, Maackiain ameliorates 6-hydroxydopamine and SNCA pathologies by modulating the PINK1/Parkin pathway in models of Parkinson's disease in *Caenorhabditis elegans* and the SH-SY5Y cell line, *Int. J. Mol. Sci.* 21 (2020) 4455.
- [51] Y. Nariai, H. Mizuguchi, T. Ogasawara, H. Nagai, Y. Sasaki, Y. Okamoto, Y. Yoshimura, H. Kitamura, N. Nemoto, H. Takeda, Fukui, Disruption of heat shock protein 90 (Hsp90)-Protein Kinase Cδ (PKCδ) interaction by (-)-maackiain suppresses histamine H1 receptor gene transcription in HeLa cells, *J. Biol. Chem.* 290 (2015) 27393–27402.
- [52] Y. Liu, W. Zeng, C. Ma, Z. Wang, C. Wang, S. Li, W. He, Q. Zhang, J. Xu, C. Zhou, Maackiain dampens osteoclastogenesis via attenuating RANKL-stimulated NF-κB signalling pathway and NFATc1 activity, *Cell. Mol. Med.* 24 (2020) 12308–12317.
- [53] S. Muruganandan, A. Ionescu, C. Sinal, At the crossroads of the adipocyte and osteoclast differentiation programs: future therapeutic perspectives, *Int. J. Mol. Sci.* 21 (2020) 2277.